NASA TECHNICAL
MEMORANDUM

NASA TM X-73,208

NASA TM X-73 208

AEROX – COMPUTER PROGRAM FOR TRANSONIC AIRCRAFT

AERODYNAMICS TO HIGH ANGLES OF ATTACK

VOLUME I – AERODYNAMIC METHODS AND PROGRAM

USERS' GUIDE

John A. Axelson

Ames Research Center
Moffett Field, Calif. 94035

February 1977

1. Report No TM X-73,208	2. Government Accession No.	3. Recipient's Catalog No
4. Title and Subtitle AEROX — COMPUTER PROGRAM FOR TRANSONIC AIRCRAFT AERODYNAMICS TO HIGH ANGLES OF ATTACK VOLUME I — AERODYNAMIC METHODS AND PROGRAM USERS' GUIDE		5. Report Date
		6. Performing Organization Code
7. Author(s) John A. Axelson		8. Performing Organization Report No. A-6927
9. Performing Organization Name and Address Ames Research Center Moffett Field, Calif. 94035		10. Work Unit No. 505-06-19
		11. Contract or Grant No.
12. Sponsoring Agency Name and Address National Aeronautics and Space Administration Washington, D. C. 20546		13. Type of Report and Period Covered Technical Memorandum
		14. Sponsoring Agency Code

15. Supplementary Notes

16. Abstract

    The theory, users' guide, test cases, and program listing are presented in the three volumes. The AEROX program estimates lift, induced-drag and pitching moments to high angles of attack (typ. 60°) for wings and for wing-body combinations with or without an aft horizontal tail. Minimum drag coefficients are not estimated, but may be input for inclusion in the total aerodynamic parameters which are output in listed and plotted formats.

17. Key Words (Suggested by Author(s)) Aerodynamics Computer programming and software	18. Distribution Statement Unlimited STAR Categories — 02		
19. Security Classif. (of this report) Unclassified	20. Security Classif. (of this page) Unclassified	21. No. of Pages 37	22. Price* $3.75

TABLE OF CONTENTS

- A E R O X -

COMPUTER PROGRAM FOR TRANSONIC AIRCRAFT AERODYNAMICS TO HIGH ANGLES OF ATTACK

VOLUME I.- AERODYNAMIC METHODS AND PROGRAM USERS' GUIDE

John A. Axelson

Ames Research Center

Summary

The theory formulated in the AEROX computer program for estimating aircraft aerodynamics to high angles of attack (60°) and a program user's guide are included in the present Volume I. Program operators concerned specifically with program execution should consult pages 15 through 19. Volume II contains comparisons of the estimated and experimental aerodynamics for nine test cases over wide ranges of angle of attack and Mach number. A program listing and sample output tables and plots are shown in Volume III.

The AEROX program estimates the coefficients of lift, induced-drag and pitching moment for wings and for wing-body combinations with or without an aft horizontal tail. Both trimmed and untrimmed characteristics are estimated. Minimum drag coefficients (e.g., friction, wave and propulsion-system additive drags) are not estimated in AEROX, but may be input as initialized coefficients for inclusion in the total aerodynamic parameters, such as lift/drag ratio. Low-speed viscous stall is not covered. Transonic airfoil calculations utilize the chordwise locations of the local limit shock waves. These designated shock locations are entered as an input parameter, rather than extracted as solutions.

The AEROX program is based on new forms of compressible wing theory covering potential and nonpotential flows, allowing for local regions of transonic limit Mach numbers, and encompassing attached and detached leading-edge shocks in supersonic flow. The program is applicable to broad ranges of configurations and flight conditions, and has a rapid computer execution time, (30 points per second on the IBM 360). It has been used extensively in computerized aircraft preliminary design and optimization studies, and would be a valuable asset in activities concerned with aerodynamic instruction, correlation and research.

INTRODUCTION

The AEROX computer program for estimating aircraft aerodynamics to high angles of attack is based on new, nonlinear foi ulations of compressible wing theory extended to cover transonic and supersonic flows, including shock waves and attendant rotational flows. The unavailabil ty of any rigorous method for calculating three-dimensional aerodynamics to high angles of attack was discussed by A.M.O. Smith in the 1974 AIAA Wright Brothers Lecture reported in reference 1. The primary obstacle cited was the continuing and current inability to define the overall influence of viscosity.

The AEROX ap; roach postulates that transonic and supersonic flows past airfoils are dominated by shock waves, and that the primary effects of viscosity are in determining the skin friction and in influencing the chordwise location of transonic shock waves. These shock locatiol.s are not extracted as solutions, but rather are entered as a designated input parameter. The effects of varying the shock location are then visible in the listed and plotted outputs of aerodynamic coefficients.

The nonpotential lift and induced drag equations are based on the integrations of momentum components in the plane through the trailing edge and normal to the flight direction. The onset of nonpotential, transonic flow around conventional, blunt airfoils is assumed to occur when the Laitone limit values for local Mach number or loading from references 2 or 3 are attained on the airfoil nose or along its surface. Additional discussion and supporting experimental evidence for this concept appear in reference 4.

The prototype program has been in operation at the Ames Research Center since 1973, (FORTRAN IV, LEVEL G), on the IBM 360 and CDC 7600 computers. It has been used in numerous aircraft preliminary-design and optimization studies, some examples of which are documented in references 5, 6 and 7. The synthesis program also included the CONMIN optimizer repciced in reference 8.

Nomenclature

The symbols used in the input-output formats, the data set listings and in the equations are identified as follows:

AEROX	program name
ALEL J, J	input integer identifying type of airfoil ($1 \leq J \leq 5$) See AXE listing
ALER, α_E	angle of attack for onset of the leading-edge limit Mach number, rad.
ALFTR, α_{TRIM}	trimmed angle of attack, deg. (ITRIM=1)
ALPHA,ALF, α	angle of attack of wing reference plane, deg.
ALTV	input altitude, ft.
AMC	maximum angle of attack for subsonic compressibility or interference (40) deg.
APLAN	planform area of nose, sq. ft.
ARDET	angle of attack for shock detachment from sharp airfoils, rad.
ARH	input aspect ratio of horizontal tail
ARW	input aspect ratio of wing
ARWX	aspect ratio of exposed wing
ASECT	nose maximum cross sectional area, sq. ft.
AT62	subroutine for atmospheric properties
AXE	subroutine for wing aerodynamics
BCLCD1	subroutine for body aerodynamics
BDMAX	input body diameter, ft.
CBARW	wing mean aerodynamic chord, ft.
CDCAM	drag coefficient due to wing camber CLO
CDHOR	induced drag coefficient of horizontal tail (ref. to SWING)
CDN	nose or body induced drag coefficient (ref. to SWING)
CDO	input minimum drag coefficient for wing (exclude camber) ICDO=1.
CDOB	input additive drag coefficient for body, tail, propulsion, ICDO= 1.
CDSEP	wing separation drag coefficient in flow zone 4
CDTOT, CD	total drag coefficient, includes CDO, CDOB when ICDO=1.
CDW , CD_i	wing induced drag coefficient
CISQ	polynomial in wing lift-curve slope equation, $SIN^4\alpha + COS^2\alpha - 2SIN^2\alpha - \frac{3}{2} SIN^2\alpha COS^2\alpha$
CLALFA	wing lift-curve slope, per deg.
CLHOR	horizontal tail lift coefficient (ref. to SWING)

CLLES   wing lower-surface lift coefficient at α_E

CLN   nose or body lift coefficient (ref. to SWING)

CLO   input wing lift coefficient at $\alpha=0$

CLOB   input additive lift coefficient for body, propulsion

CLTOT, CL   total lift coefficient

CLW   wing lift coefficient

CLWL   lift coefficient for wing lower surface

CLWU   lift coefficient for wing upper surface

CLUBS   incremental wing lift coefficient of upper surface in interval $\alpha - \alpha_E$

CLUES   wing upper surface lift coefficient at α_E

CM, C_m pitching-moment coefficient

CMO   input wing pitching-moment coefficient at $\alpha=0$.

CMOB   input additive pitching-moment coefficient for body (BCLCD1 subroutine)

CPDS   pressure coefficient downstream of limit shock for Z=4 (IXCD=0)

CPLIM   limit pressure coefficient

CPMXS   pitot compressibility factor for lower surface lift ($Z \leq 4$)

CPSTAG   stagnation pressure coefficient behind normal shock (Z=6)

CP2   pressure coefficient downstream of limit shock for Z=4 (IXCD=1)

CROOT   wing root chord ($\mathcal{l}$), ft. (streamwise)

CTIP   wing tip chord, ft. (streamwise)

DALTR   adjustment of angle of attack for trim at constant C_L, deg.

DCDTR   incremental trim drag coefficient

DCLTR   increment of lift coefficient during trim

DDISP   plot control integer for component drag coefficients; 0, No plot, 1, plot printed

DELH   increment of horizontal-tail deflection to trim, deg.

DEPDA   rate of change of downwash angle with angle of attack

DEXP   exponent in induced drag coefficient equation, $1.5 - \dfrac{M\cos \overline{SWPWLF}}{4}$ for M 1; $1.5 - \dfrac{M^2 \cos SWPWLF}{4}$ for 1 M.

DLWING, $\dfrac{dCL}{d\alpha}$ wing lift-curve slope, per rad.

DNBL   Mach number attenuation factor for lift-curve slope in Z=6

DWASH, EPS1   downwash angle at the designated horizontal tail location, deg.

Nomenclature - Page 3

ED	eccentricity of wing CBARW/4; XQMAC-XCG
EPSD	wake downwash angle
FDNOSE	multiplying factor for nose drag, programmed unity
FINT	wing-body interference factor, attenuated with α, $Z \leq 4$, $M \leq 1.4$
FLAX	wing-body interference factor, $5 \leq Z$
FLEX	lift factor for wing chord extension
FLNOSE	multiplying factor for nose lift, programmed unity
FMOML	wing lower-surface lift factor for $Z=6$
FMOMU	wing upper-surface lift factor for $Z=6$
FTOTD	multiplying factor for change of reference area for C_D
FTOTL	multiplying factor for change of reference area for C_L
FCM	multiplying factor for change of reference dimensions for C_M
GEOM1	subroutine for calculating geometric parameters
ICDO	input control integer for minimum drag; 0, CDO omitted; 1, input wing CDO included
IDATA	input control integer on printout; 0, no print; 1, listing printed
IFLEX	input control integer for strake bluntness; 0, sharp; 1, blunt
IPLOT	input control integer for plots; 0, no plots; 1, plots printed
ITABL	input control integer for geometry heading; 0, no print; 1, heading printed
ITRIM	input control integer for trim option; 0, data untrimmed; 1, trimmed
IT	input horizontal-tail incidence, deg.
IXCD	input control integer for limit shock position; 0, constant X/C; 1, limit shock sweep angle SHK specified from XCD at airplane centerline
J,ALELJ	input integer identifying type of airfoil - See AXE listing
L/D	lift/drag ratio, when ICDO-1.
LDISP	input plot-control integer; 0, no plot; 1, component lift coefficient plotted
LE	tail length from moment center, ft.; XQHOR-XCG
LT	tail length from CBARW/4, ft.; XQHOR-XQMAC
M, SMN	Mach number
Mc	cross-flow Mach number, $M \sin\alpha$ in BCLCD1 subroutine; fig. 3.
MPLOT	subroutine for trimmed plots, all Mach numbers together.
P_2	static pressure downstream of limit shock
PLOT	subroutine for untrimmed plots, plot set for each M.
PPLOT	input plot-control integer; 0, + Cm right; 1, + Cm left
P_{T_1}	free-stream stagnation pressure

RNC	body cross-flow Reynolds number; fig. 3.
RNLOC	Reynolds number per foot for input Mach number and altitude.
ROC	input leading-edge radius to chord ratio for J=5 airfoils.
SEXT	input area of wing chord extension (forward strake), sq. ft.
SHK	input sweep angle of the limit shock in Z=4 with IXCD=1, deg.
SHOR	input horizontal tail area, sq. ft.
SMN,M	Mach number
SPANW	wing span, ft.
SQH	input sweep angle of horizontal-tail C/4 line, deg.
SQW;SWPW	input sweep angle of wing C/4 line, deg.; rad.
SWING	input wing reference area, sq. ft.
SWPWLE	Sweep angle of the wing leading edge, rad.
SX	exposed wing area, sq. ft.
SXC;SHK	sweep angle of limit shock, Z=4, IXCD=0;1.
TCRW	input thickness-to-chord ratio of wing $\bar{c}$ (streamwise)
TCTW	input thickness-to-chord ratio of wing tip chord (streamwise)
TRIMDG	subroutine for downwash, tail aerodynamics and trim
TRW	input wing taper ratio, CTIP/CROOT
XCD, X/C	input chordwise location of limit shock, Z=4.
XCG	input longitudinal station of moment center (or CG), ft.
XEXT	input longitudinal station of centroid of wing chord extension SEXT, ft.
XLB	input body length, ft.
XLN	input nose length, ft.
XQHOR	input longitudinal station of horizontal-tail C/4, ft.
XQMAC	input longitudinal station of wing CBARW/4, ft.
Y	vertical coordinate
YBAR	lateral station of the wing mean aerodynamic chord, ft.
YHOR	input height of horizontal tail from wing plane, positive for high tail, ft.
Z	integer identifying flow zone
α, ALPHA	angle of attack of wing reference plane, deg.
α_E, ALER	angle of attack for onset of the leading-edge limit Mach number, rad.
γ	ratio of specific heats for air, 1.4.
α_H	horizontal-tail angle of attack
	bar over a parameter denotes the effective value; e.g.,

$$\overline{SQW} = SIN^{-1}[SIN(SQW)COS(\alpha)]$$

AERODYNAMIC THEORY

The equations for evaluating airfoil aerodynamics are organized according to the division of the flight envelope into the flow zones depicted in figure 1. The cross-hatched viscous stall region is not included in the present method. The flow is considered incompressible for Mach numbers below 0.1. The compressible, shockless zone 2 covers airfoils with blunt leading edges and with surrounding flows having local Mach numbers everywhere below the Laitone limit value ($SQRT(\gamma+3)/2$). The boundary between zones 2 and 3 is estimated by the equation for ALER, the angle of attack for onset of the limit Mach number at the leading edge. The onset of the surface limit-Mach number, zone 4, occurs when the upper-surface lift for zone 2 or 3 reaches the limit lift corresponding to the designated chordwise shock location, XCD. Sharp airfoils are considered to have reached the leading-edge Mach limit for all subsonic flow, and are treated with the nonpotential lift equations of zones 3 and 4. Zone 5 applies only to sharp airfoils having supersonic leading edges with attached shocks. Finally, flow zone 6 covers all airfoils with detached, leading-edge shocks. The supersonic leading edges for zones 5 and 6 occur when the normal component of Mach number exceeds unity (M cos $\overline{SWPWLE} \geq 1.$).

The following equations apply to an equivalent wing having straight leading and trailing edges. Account is made for strakes and wing forward-chord extensions in AEROX by multiplying all of the following equations for lift coefficient and wing lift-curve slope by the term (1 + FLEX). FLEX, the empirical lift factor for the chord extension, is defined within the program and depends on Mach number, angle of attack, and whether the extension is sharp (IFLEX=0) or blunt (IFLEX=1).

Incompressible Flow Zone 1 (M<0.1)

The incompressible lift equation for conventional airfoils is taken from the potential-flow theory of Kutta-Joukowski. The lift equation for nonpotential flow, such as around sharp airfoils, is based upon the integration of downwash momentum. Both equations are extended to three-dimensional flows through the inclusions of the Prandtl aspect-ratio transformation and the cosine term involving the effective sweep of the quarter-chord line. The potential-flow equations for conventional airfoils are:

$$C_L = 2\pi \sin\alpha \cos \overline{SQW} \left(\frac{ARW}{ARW+2}\right) \tag{1}$$

$$\frac{dC_L}{d\alpha} = 2\pi \cos\alpha \cos \overline{SQW} \left(\frac{ARW}{ARW+2}\right) \tag{2}$$

$$C_{D_i} = \frac{C_L^2}{\pi\,ARW} \tag{3}$$

The nonpotential equations derived in the Appendix are:

$$C_L = 2\pi \sin\alpha\cos^2\alpha \left(1 - \frac{\sin^2\alpha}{2}\right)\cos \overline{SQW} \left(\frac{ARW}{ARW+2}\right) \tag{4}$$

$$\frac{dC_L}{d\alpha} = \pi\cos\alpha\,(2\sin^4\alpha + 2\cos^2\alpha - 4\sin^2\alpha - 3\sin^2\alpha\cos^2\alpha)\cos \overline{SQW}\left(\frac{ARW}{ARW+2}\right) \tag{5a}$$

$$= 2\pi\cos\alpha(CISQ)\cos \overline{SQW} \left(\frac{ARW}{ARW+2}\right) \tag{5b}$$

$$C_{D_i} = C_L(TAN\ )^{DEXP} \tag{6}$$

The incompressible lift is comprised of equal contributions from the upper and lower wing surfaces. The nonpotential equations asymptotically approach the potential equations at small angles of attack.

Compressible, Shock-free Flow Zone 2

In estimating the aerodynamics for airfoils having subsonic leading edges, separate compressibility factors are used for the lifts of the upper and lower surfaces. For compressible, shock-free flow (zone 2) on the upper surface of

8

blunt airfoils, a Prandtl-Glauert factor is used involving the component of flight Mach number normal to the quarter-chord line and an angle-of-attack attenuation to value unity at 40°.

$$\bar{F}_u = \frac{1-\left(1-\sqrt{1-M^2\cos^2 \overline{SQW}}\right)\left(\frac{\alpha}{40}\right)^2}{\sqrt{1-M^2\cos^2 \overline{SQW}}} \qquad (7)$$

No compressibility factor is used for the upper-surface lift in nonpotential flow, because the onset of the local Mach-limit is considered to "freeze" the local flow.

Lower-surface lifts in potential and nonpotential flows around airfoils having subsonic leading edges are evaluated using a pitot-compressibility factor expressing the ratio of the leading-edge, stagnation-line pressure in compressible flow to that in incompressible flow. Account is included for variations in the angles of attack and sweep, and for wing-body interference patterned after the FLAX parameter from references 9 and 10.

$$\bar{F}_\ell = CPMXS = \frac{1}{\gamma M^2 \cos^2 \overline{SWPWLE}}\left\{\left[1+\left(\frac{\gamma-1}{2}\right)(FINT)M^2\cos^2\overline{SWPWLE}\right]^{\frac{\gamma}{\gamma-1}}-1\right\} \qquad (8)$$

$$FINT = \left[1+\left(1-\frac{\alpha}{40}\right)^2\frac{BDM}{SPAN}\right. \qquad (M\leq1) \qquad (8a)$$

$$= \left\{1+\left[1-\left(\frac{\alpha}{40}\right)\left(\frac{1.4-M}{0.4}\right)\right]^2\frac{BDMAX}{SPANW}\right\}^2 \qquad (1\leq M\leq1.4) \qquad (8b)$$

$$= \left(1+\frac{BDMAX}{SPANW}\right)^2 \qquad (1.4\leq M) \qquad (8c)$$

The compressible, potential-flow equations for conventional airfoils are obtained by incorporating the compressibility factors, equations (7) and (8), into equations (1) and (2).

$$C_L = \left[\bar{F}_U(\text{FINT}) + \bar{F}_\ell\right] \pi \sin\alpha \cos\overline{\text{SQW}}\left(\frac{\text{ARW}}{\text{ARW}+2}\right) \quad (9)$$

$$\frac{dC_L}{d\alpha} = \left[\left(\bar{F}_U \cos\alpha + \frac{d\bar{F}_U}{d\alpha}\sin\alpha\right)(\text{FINT}) + \bar{F}_\ell \cos\alpha\right] \pi \cos\overline{\text{SQW}}\left(\frac{\text{ARW}}{\text{ARW } 2}\right) \quad (10)$$

$$C_{D_i} = \frac{C_L^2}{\pi \text{ARW}} \quad (3)$$

Sharp airfoils in subsonic, compressible flow are treated as nonpotential, Mach-limited flows, and assigned to flow zones 3 or 4.

Leading-edge Mach-limited Flow Zone 3

The onset of the Laitone limit Mach number in the curvilinear flow around a blunt-airfoil leading edge is estimated by the value of the onset angle of attack, α_E, derived as equation (A11), in the Appendix. A brief discussion of the conceptual flow model undergoing the transition from compressible, potential flow to Mach-limited, nonpotential flow follows.

After attaining the local limit Mach number around the leading edge, further increases in angle of attack or in flight Mach number tend to enlarge the local Mach-limited region on the airfoil nose. The enlargement of the constant velocity profile in the curvilinear flow around the nose disrupts the radial equilibrium between the local,radial static-pressure gradient and the local,centrifugal forces. (Irrotational, curvilinear flow exists only when radial equilibrium prevails,which requires an essentially inverse relationship between local velocity and local streamline radius of curvature.) The constant-velocity profile may be accompanied by the dominance of the local centrifugal forces and the possible formation of a separation bubble. When the locally supersonic flow decelerates (and reattaches) just downstream of the nose (with or without the separation bubble), a "peaky" pressure distribution results, (shown in ref. 4). This flow is designated in AEROX as leading-edge Mach-limited, or zone 3. When the separation bubble is present, the mixing action of the rotational-flow layers emenating from the disrupted nose flow may promote the flow reattachment.

When the supersonic limit-Mach number extends well back on the airfoil upper surface, resulting in the flat pressure distribution (also in ref. 4), the flow is surface Mach-limited, and assigned to zone 4. Surface Mach-limited flow is modeled to have separation downstream of the surface limit shock, resulting in an additive drag component, CDSEP. Experimental confirmation of the separation appears in pressure distributions, samples of which were included in reference 4.

Sharp airfoils in compressible, subsonic flow are treated as leading-edge Mach-limited flow with the nonpotential zone 3 equations.

$$C_L = \left(1 + \bar{F}_{\ell}\right) \pi \sin\alpha \cos^2\alpha \left(1 - \frac{\sin^2\alpha}{2}\right) \cos \overline{SQW} \left(\frac{ARW}{ARW+2}\right) \tag{11}$$

$$\frac{dC_L}{d\alpha} = \left(1 + \bar{F}_{\ell}\right) \pi \cos\alpha \left(CISQ\right) \cos \overline{SQW} \left(\frac{ARW}{ARW+2}\right) \tag{12}$$

$$C_{D_i} = C_L \left(\tan\alpha\right)^{DEXP} \tag{13}$$

The lift curves for blunt airfoils traversing from compressible, potential flow (zone 2) into zone 3 are assigned a continuous mathematical transition, rather than a discontinuous jump, so that the program may be coupled to an optimizer program. The lift equation is the sum of the zone 2 lift (eq. (9)) evaluated at α_E and an incremental lift for the interval $(\alpha - \alpha_E)$ in zone 3, until eq. 11 is reached.

$$C_L = \text{Greater of} \begin{cases} \left[\bar{F}_V (FINT) + \bar{F}_{\ell}\right] \pi \sin\alpha_E \cos \overline{SQW} \left(\frac{ARW}{ARW+2}\right) + \left(\frac{dC_{L_V}}{d\alpha} + \frac{dC_{L_{\ell}}}{d\alpha}\right)(\alpha - \alpha_E) \\ Eq.(11) \end{cases} \tag{14}$$

Surface Mach-limited Zone 4

The conceptual flow model depicting surface Mach-number limited flow past an airfoil is shown in figure 2. The Laitone limit Mach number (refs. 2, 3) corresponds to the maximization of the static pressure behind the surface limit shock.

$$\frac{d\left(\frac{P_2}{P_{T_1}}\right)}{dM_{Loc}} = 0 \quad ; \quad M_{LIM} = \sqrt{\frac{\delta+3}{2}} \tag{15}$$

11

This criterion is extended to swept wings in the AEROX program with the
following limit pressure coefficient.

$$C_{P_{LIM}} = \frac{2}{\delta M^2} \left\{ \frac{\left[1 + \left(\frac{\gamma-1}{2}\right) M^2 \cos^2 \overline{SXC} \right]^{\frac{\gamma}{\gamma-1}}}{3.58} - 1 \right\} \tag{16}$$

The airfoil lift coefficient for zone 4 is the sum of the lower-surface
nonpotential lift (eq. (11) and the upper-surface limit lift, which is
dependent upon the designated chordwise location, XCD of the surface limit
shock. The program uses XC = f(XCD) which moves the limit shock to the trailing
edge as the sonic leading-edge condition is reached.

$$C_L = - \left[C_{P_{LIM}}(XC) + \frac{1}{2} C_{P_{DS}}(1-XC) \right] \cos\alpha + \bar{F}_\gamma \, \pi \sin\alpha \, \cos^2\alpha \left(1 - \frac{\sin^2\alpha}{2} \right) \cos \overline{SQW} \left(\frac{ARW}{ARW+2} \right) \tag{17}$$

$$\frac{dC_L}{d\alpha} = \left[C_{P_{LIM}}(XC) + \frac{1}{2} C_{P_{DS}}(1-XC) \right] \sin\alpha + \bar{F}_\gamma \, \pi \, \cos\alpha \, (CISQ) \cos \overline{SQW} \left(\frac{ARW}{ARW+2} \right) \tag{18}$$

$$C_{D_i} = \frac{C_L^2}{\pi ARW} + C_L (\tan\alpha)^{DEXP} + C_{D_{SEP}} \tag{19}$$

CPDS is the pressure coefficient downstream of the limit shock, corresponding
to p_2 in figure 2. The separation drag coefficient, $C_{D_{SEP}}$, accounts for the
momentum deficit in the modeled separation wake passing the trailing edge.
The wake is assumed to originate at the base of the limit shock, to have its
upper edge follow a line inclined at one-half the angle of attack, and to have
a linear velocity profile between the zero value on the surface to the free-
stream value at the upper edge.

$$C_{P_{DS}} = \frac{2}{\delta M^2} \left[\left\{ \frac{2\gamma \left[\left(\frac{\gamma+3}{2} \right) + M^2 \sin^2 \overline{SXC} \right] \cos^2 \overline{SXC} - (\gamma-1)}{\gamma+1} \right\} \left\{ \frac{2 \left[1 + \left(\frac{\gamma-1}{2} \right) M^2 \right]}{(\gamma-1) \left[\left(\frac{\gamma+3}{2} \right) + M^2 \sin^2 \overline{SXC} + 2 \right]} \right\}^{\frac{\gamma}{\gamma-1}} - 1 \right]$$

$$C_{D_{SEP}} = (SPANW - BDMAX)(1-XC) \left(\frac{CBARW}{SWING} \right) \left(\frac{\sin\alpha}{2} \right)$$

Supersonic Attached-Shock Zone 5

Airfoils having sharp leading edges with attached shocks are treated in

zone 5. The upper boundary is the angle of attack for shock detachment, ARDET, which is evaluated by equations based on curve-fitting figure 4 in reference 11 for supersonic speeds, and based on the theory of reference 12 for hypersonic speeds. The supersonic lift coefficients are estimated by the nonpotential equation (11) using the exposed wing area, an empirical, Mach-attenuated aspect-ratio transformation, and the wing-body interference factor of Flax (ref. 9, 10) applied to the lower surface lift.

$$C_L = 2\pi \sin\alpha \cos^2\alpha \left(1 - \frac{\sin^2\alpha}{2}\right)\left(\frac{ARWX}{ARWX + \frac{2}{M}}\right)\left(\frac{Sx}{SWING}\right)\left[FLAX\left(1 - \frac{.65}{M}\right) + \frac{.65}{M}\right] \qquad \left(M \leq \sqrt{2}\right) \qquad (20)$$

$$\frac{dC_L}{d\alpha} = 2\pi \cos\alpha \, (CISQ)\left(\frac{ARWX}{ARWX + \frac{2}{M}}\right)\left(\frac{Sx}{SWING}\right)\left[FLAX\left(1 - \frac{.65}{M}\right) + \frac{.65}{M}\right] \qquad \left(M \leq \sqrt{2}\right) \qquad (21)$$

For $\sqrt{2} < M \leq 3$, multiply the above equations by $(M^2 - 1)^{-1/2}$

At Mach numbers above 3, lift coefficients are evaluated by the explicit, oblique-shock theory of reference 12.

$$C_L = \left(\frac{2}{\delta + 1}\right)\left(\frac{Sx}{SWING}\right)\left(\frac{ARWX}{ARWX + \frac{2}{M}}\right)\left(1 + \delta \sin^2\alpha - \cos\alpha \sqrt{1 - \frac{4}{M^2}\left(\frac{\alpha}{16}\right) - \delta^2 \sin^2\alpha}\right)\cos\alpha \qquad \left(\alpha \leq 16°; \, 3 < M\right) \qquad (22a)$$

$$C_L = \left(\frac{2}{\delta + 1}\right)\left(\frac{Sx}{SWING}\right)\left(\frac{ARWX}{ARWX + \frac{2}{M}}\right)\left(1 + \delta \sin^2\alpha - \cos\alpha \sqrt{1 - \frac{4}{M^2} - \delta^2 \sin^2\alpha}\right)\cos\alpha \qquad \left(16 < \alpha < \alpha_{DET}; \, 3 < M\right) \qquad (22b)$$

$$\frac{dC_L}{d\alpha} = \left(\frac{Sx}{SWING}\right)\left[\left(\frac{2}{\delta + 1}\right)\left(2\delta \sin\alpha \cos^2\alpha + \sin\alpha \cos\alpha \sqrt{1 - \frac{4}{M^2} - \delta^2 \sin^2\alpha} + \frac{\delta^2 \sin\alpha \cos^3\alpha}{\sqrt{1 - \frac{4}{M^2} - \delta^2 \sin^2\alpha}}\right)\left(\frac{ARWX}{ARWX + \frac{2}{M}}\right) - C_L \tan\alpha\right] \qquad (3 < M)$$

$$(23)$$

$$C_{D_i} = C_L \tan\alpha \qquad (24)$$

Supersonic Detached-Shock Zone 6

Blunt airfoils with supersonic leading edges and sharp airfoils with detached leading-edge shocks are treated with the following equations combining the nonpotential equation (11) derived from diverted momentum and modified Newtonian impact theory, which assumes increased importance on the windward surface loading at hypersonic speed. The limit pressure coefficient for the upper surface undergoes a transition from a value of -0.68 at M=1 and approaches the value $-\frac{1}{M}2$, the well-known empirical value suggested by MAYER in reference 13.

$$C_{P_{LIM}} = -\frac{1}{M^2}\left(1 - \frac{.32}{M^{2.5}}\right) \tag{25}$$

The upper surface lift coefficient becomes a small fraction of the total lift coefficient as Mach number increases.

$$C_{L_U} = LESSER\ OF \begin{cases} -C_{P_{LIM}}\left(\frac{S_x}{S_{WING}}\right)\cos\alpha \\ \pi\sin\alpha\cos^2\alpha\left(1-\frac{\sin^2\alpha}{2}\right)\left(\frac{S_x}{S_{WING}}\right)\left(\frac{ARWX}{ARWX+\frac{2}{M}}\right)\left(\frac{FMOMU}{DNBL}\right) \end{cases} \tag{26 a,b}$$

$$C_{L_\ell} = \pi\sin\alpha\cos^2\alpha\left(1-\frac{\sin^2\alpha}{2}\right)\left(\frac{S_x}{S_{WING}}\right)\left(\frac{ARWX}{ARWX+\frac{2}{M}}\right)\left(\frac{FMOML}{DNBL}\right)(FLAX)C_{P_{STAG}} + C_{P_{STAG}}\sin^2\alpha\cos\alpha \tag{27}$$

$$\frac{dC_{L_U}}{d\alpha} = LESSER\ OF \begin{cases} C_{P_{LIM}}\left(\frac{S_x}{S_{WING}}\right)\sin\alpha \\ \pi\cos\alpha(CISQ)\left(\frac{ARWX}{ARWX+\frac{2}{M}}\right)\left(\frac{S_x}{S_{WING}}\right)\left(\frac{FMOMU}{DNBL}\right) \end{cases} \tag{28a,b}$$

$$\frac{dC_{L_\ell}}{d\alpha} = \pi\cos\alpha(CISQ)\left(\frac{ARWX}{ARWX+\frac{2}{M}}\right)\left(\frac{S_x}{S_{WING}}\right)\left(\frac{FMOML}{DNBL}\right)(FLAX)C_{P_{STAG}} + C_{P_{STAG}}\sin\alpha\left(2\cos^2\alpha-\sin^2\alpha\right) \tag{29}$$

$$C_L = C_{L_U} + C_{L_\ell} \ ; \quad \frac{dC_L}{d\alpha} = \frac{dC_{L_U}}{d\alpha} + \frac{dC_{L_\ell}}{d\alpha}$$

$$C_{D_i} = C_L \tan\alpha \tag{24}$$

The empirical constants entering the diverted-momentum (nonpotential) lift contribution include DNBL, establishing the variation with Mach number, and

14

FMOMU and FMOML, expressing the division of the diverted momentum lift to the upper and lower wing surfaces.

$$DNBL = \begin{cases} M^{2/3} & (M \leq 1.77) \\ \dfrac{M^{2/3}}{\sqrt{M^2-1}} & (1.77 < M) \end{cases}$$

$$FMOMU = \begin{cases} 1. & (M \leq 1.2) \\ \dfrac{1.}{M-.2} & (1.2 < M) \end{cases}$$

$$FMOML = \begin{cases} 1.6 - .6M & (M \leq 1.5) \\ 0.7 & (1.5 < M \leq 2.2) \\ 0.1 + \dfrac{1}{M-.55} & (2.2 < M) \end{cases}$$

APPLICATION TO AIRCRAFT CONFIGURATIONS

Input

Input file formats for the IBM 360 and CDC 7600 computers are enclosed. Each item is discussed here and also identified in the nomenclature. Note that parametric studies may be performed by entering the minimum and maximum values and increments for the wing aspect ratio (ARW), wing taper ratio (TRW), wing quarter-chord sweep angle (SQW), angle of attack (ALF), and the designated chordwise shock locations (XCD). For a particular airplane or single value to any of these parameters, enter the value as the minimum and the maximum, and

15

assign an appropriate non-zero value for the increments, (see sample input sheets for test cases in vol. II). The program allows an array of up to (I) twenty Mach numbers and up to (K) twenty angles of attack. Angles of attack to 40° are usually input as 2° minimum, 40° maximum, with 2° increments. Angles to 80° can be input as 4° minimum, 80° maximum, with 4° increments. Maximum angles should not reach 90°. Enter dataset title, (see input format).

NSMN	number of Mach numbers in the array, up to 20.
SMN	list the Mach numbers in the array.
ICDO	input control integer for minimum drag; 0, CDO omitted; 1, input value of CDO included in CDTOT and L/D.
CDO	input CDO values for each Mach number in the array.
CMO	input CMO values for each Mach number in the array.
CLOB	input CLOB values for each Mach number in the array.
CDOB	input CDOB values for each Mach number in the array.
CMOB	input CMOB values for each Mach number in the array.
ITRIM	input control integer for trim option; 0, untrimmed; 1, trimmed.
ALELJ	input airfoil identification integer; 1, sharp; 2, NACA 230XX and 00XX airfoils; 3, NACA 6 series airfoils; 4, slab airfoils with round leading edges; 5, leading-edge radius-to-chord ratio specified.
MNARW	minimum wing aspect ratio
MXARW	maximum wing aspect ratio
INARW	incremental wing aspect ratio
MNTRN	minimum wing taper ratio
MXTRW	maximum wing taper ratio
INTRW	incremental wing taper ratio
MNSQW	minimum wing quarter-chord sweep angle, deg.
MXSQW	maximum wing quarter-chord sweep angle, deg.
INSQW	incremental wing quarter-chord sweep angle, deg.
SWING	wing reference area for equivalent wing having straight leading and trailing edges, sq. ft.
TCRW	streamwise thickness-to-chord ratio at wing centerline
TCTW	streamwise thickness-to-chord ratio at wing tip
ROC	leading-edge radius-to-chord ratio; specify for ALELJ=5; otherwise, zero.
SEXT	area of wing chord forward extensions or strakes, sq. ft.
XEXT	longitudinal station of centroid of chord extensions, ft.
IFLEX	input 0 for sharp chord extensions, 1 for blunt.

BDMAX	maximum body diameter, ft.
XLN	nose length, ft. (longit. 0 station at nose)
XLB	body length, ft.
XCG	longitudinal station of moment center or center of gravity, ft.
SHOR	horizontal tail area, sq. ft.
XQHOR	longitudinal station of horizontal tail C/4 line, ft.
ARH	aspect ratio of horizontal tail
SQH	sweep angle of C/4 line of horizontal tail, deg.
YHOR	vertical height of tail from wing plane, ft. (+ tail above plane)
IT	horizontal tail incidence, deg.
MNALF	minimum angle of attack, deg. (usually 2°)
MXALF	maximum angle of attack, deg. (usually 40°)
INALF	incremental angle of attack, deg. (usually 2°)
MNXCD	most forward chord location of limit shock in Z=4, (typ. .3)
MXXCD	most rearward chord location of limit shock in Z=4, (max 1.)
INXCD	incremental fraction of chord for intermediate shock locations.
IXCD	control integer; 0, limit shock in Z=4 is at constant fraction of chord across the wing span; 1, limit shock starts at XCD at $\cancel{}$, extends outboard at the specified limit shock sweep angle, SHK.
SHK	limit shock sweep angle, deg. for IXCD=1; 0 for IXCD=0.
ALTV	altitude, ft.
FTOTL	multiplying factor for change of lift coefficient reference area (def.1.)
FTOTD	multiplying factor for change of drag coefficient reference area (def.1.)
FCM	multiplying factor for change of pitching-moment coefficient reference dimensions
IDATA	listing-control integer; 0, no print; 1, printout provided.
ITABL	listing-control integer; 0, no heading; 1, heading printed.
IPLOT	plot-control integer; 0, no plot; 1, plots provided.
PPLOT	0, + CM plotted to right; 1, + CM to left.
LDISP	component lift-coefficient plot control integer; 0, no plot; 1, plot provided. Six outputs are CLHOR, CLN, CLWL, CLWU, CLW, CLTOT
DDISP	component drag-coefficient plot-control integer; 0, no plot; 1, plot provided. Four outputs are CDN, CDSEP, CDW, CDTOT

In addition to sweep angle, SQW, at least three additional wing planform parameters must be specified: SWING, ARW, and TRW. The program calculates the following parameters if they are input as zero: SPANW, CROOT, CTIP, CBARW, YBAR. Also, for a wing alone having longitudinal station 0, at the leading-edge

apex, the program calculates XQMAC, if it is input as zero. For all other cases, XQMAC must be input. The choice of horizontal tail area depends on the tail configuration. Use total planform area for large tails on small afterbodies. With wide bodies enclosing twin jets, use exposed tail area.

AEROX includes the following subroutines:

1. AEROX   Driver control, read and write statements
2. AT62   Atmospheric properties
3. GEOM1   Geometric parameters
4. AXE   Wing aerodynamics and configuration totals
5. BCLCD1   Body aerodynamics
6. TRIMDG   Tail aerodynamics, C_M, trim
7. PLOT   Untrimmed C_L vs. α, C_L vs. C_D, C_L vs. C_M for each M
8. MPLOT   Trimmed C_L vs. α, C_L vs. C_D, all M's together

IBM 360 INPUT FORMAT

```
COLUMN 2
    |
    v

    TITLE UP TO 56 CHARACTERS LONG
    &ARRAYS
    NSMN    •
    SMN     •
    ICDO    •
    CDO     •
    CMO     •
    CLOB    •
    CDOB    •
    CMOB    •
    ITRIM   •
    &END

    &WINGIN
    ALELJ   •       •
    MNARW   •       •   MXARW   •       •   INARW   •       •
    MNTRW   •       •   MXTRW   •       •   INTRW   •       •
    MNSOW   •       •   MXSOW   •       •   INSOW   •       •   CLO     •           •
    SWING   •       •   SPANW   •       •   CROOT   •       •   CTIP    •           •
    TCRW    •       •   TCTW    •       •   XOMAC   •       •   CBARW   •           •
    ROC     •       •   SEXT    •       •   XEXT    •       •   IFLEX   •           •
    &END

    &NOSEIN
    BDMAX   •       •   XLN     •       •   XLB     •       •   XCG     •           •
    &END

    &TAILIN
    SHOR    •       •   XOMOR   •       •   ARH     •       •   SOH     •           •
    YHOR    •       •   IT      •       •
    &END

    &FLOWIN
    MNALF   •       •   MXALF   •       •   INALF   •       •
    MNXCD   •       •   MXXCD   •       •   INXCD   •       •
    IXCD    •       •   SHK     •       •
    ALTV    •       •
    &END

    &FACTOR
    FTOTL   •       •   FTOTD   •       •   FCM     •       •
    &END

    &OUTPUT
    IDATA   •   •   ITABL   •       •
    IPLOT   •   •   PPLOT   •       •
    LDISP   •   •   •   •   •   •   •
    DDISP   •   •   •   •   •
    &END
```

COLUMN 2
↓

```
0000100   TITLE UP TO 56 CHARACTERS LONG
0000200   $ARRAYS
0000300   NSMN   ■   ,
0000400   SMN    ■   ,        , ... ,           ,(COMMA NUMBER 20)
0000500   ICDO   ■   ,        , ... ,           ,   "      "      "
0000600   CDD    ■   ,        , ... ,           ,   "      "      "
0000700   CMD    ■   ,        , ... ,           ,   "      "      "
0000800   CLDB   ■   ,        , ... ,           ,   "      "      "
0000900   CDDB   ■   ,        , ... ,           ,   "      "      "
0001000   CMDB   ■   ,        , ... ,           ,   "      "      "
0001100   ITRIM  ■   ,        , ... ,           ,   "      "      "
0001200   $END
0001300   $WINGIN
0001400   ALELJ  ■       ,
0001500   MNARW  ■       ,   MXARW  ■      ,   INARW  ■      ,
0001600   MNTRW  ■       ,   MXTRW  ■      ,   INTRW  ■      ,
0001700   MNSOW  ■       ,   MXSOW  ■      ,   INSOW  ■      ,   CLO    ■      ,
0001800   SWING  ■       ,   SPANW  ■      ,   CROOT  ■      ,   CTIP   ■      ,
0001900   TCRW   ■       ,   TCTW   ■      ,   XQMAC  ■      ,   CBARW  ■      ,
0002000   ROC    ■       ,   SEXT   ■      ,   XEXT   ■      ,   IFLEX  ■      ,
0002100   $END
0002200   $NOSEIN
0002300   BDMAX  ■       ,   XLN    ■      ,   XLB    ■      ,   XCG    ■      ,
0002400   $END
0002500   $TAILIN
0002600   SHOR   ■       ,   XQHOR  ■      ,   ARH    ■      ,   SOH    ■      ,
0002700   YHOR   ■       ,   IT     ■      ,   ,
0002800   $END
0002900   $FLOWIN
0003000   MNALF  ■       ,   MXALF  ■      ,   INALF  ■      ,
0003100   MNXCD  ■       ,   MXXCD  ■      ,   INXCD  ■      ,
0003200   IXCD   ■       ,   SHK    ■      ,
0003300   ALTV   ■       ,
0003400   $END
0003500   $FACTOR
0003600   FTOTL  ■       ,   FTOTD  ■      ,   FCM    ■      ,
0003700   $END
0003800   $OUTPUT
0003900   IDATA  ■   ,   ITABL  ■   ,
0004000   IPLOT  ■   ,   PPLOT  ■   ,
0004100   LDISP  ■   ,   ,   ,   ,   ,   ,
0004200   DDISP  ■   ,   ,   ,   ,   ,
0004300   $END
```

Nine additional cards, starting at column 7, are required for CDC 7600 operation:

At front of deck:

```
PROGRAM AEROX (INPUT, OUTPUT, TAPE5 = INPUT, TAPE 6 = OUTPUT)
```

At end of deck:

```
FUNCTION ARSIN (A)
ARSIN = A SIN(A)
RETURN
END
FUNCTION COTAN (A)
COTAN = 1./TAN (A)
RETURN
END
```

APPENDIX A - WING (AXE subroutine)
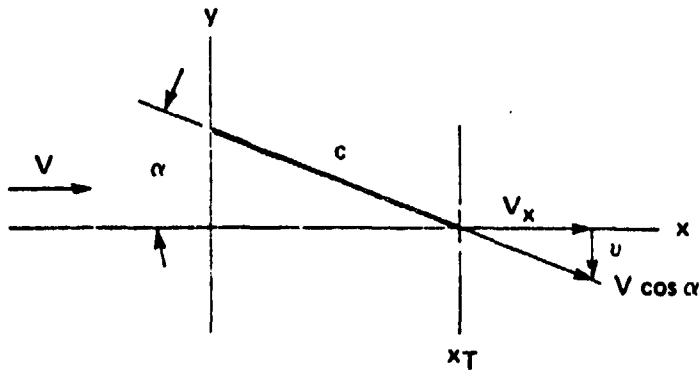### Derivation of Nonpotential Lift Equation

A description of the conceptual transonic-flow airfoil model (fig. 2)
involving local limit Mach numbers, shock waves, rotational flow and separation
is included in the text under flow - zone 3. The lift no longer conforms to
potential theory, but rather is evaluated in AEROX by equations based on the
integration of the downwash momentum in the plane passing through the airfoil
trailing edge and normal to the flight direction. The distribution of the
downwash velocity in the vertical plane is defined by the nondimensional
attenuation factor appearing in the brackets of equation (A2) below. This
factor prescribes the distribution of the disturbance velocity in the XT plane
for rectilinear flow with superposed circulation (vortex). It also closely
represents the distribution of the downwash velocity in the same XT plane also
passing through the trailing edge of the cambered, streamline airfoil shown in
the upper sketch. This factor also prescribes the distribution of the distur-
bance velocities in the two components in the XT plane through the trailing
edge of the planar airfoil shown in the lower sketch. The trailing edge
velocity $V\cos\alpha$ satisfies the assigned boundary conditions of free-stream
velocity at $\alpha=0°$ and of zero lift at $\alpha=0°$ and $\alpha=90°$.
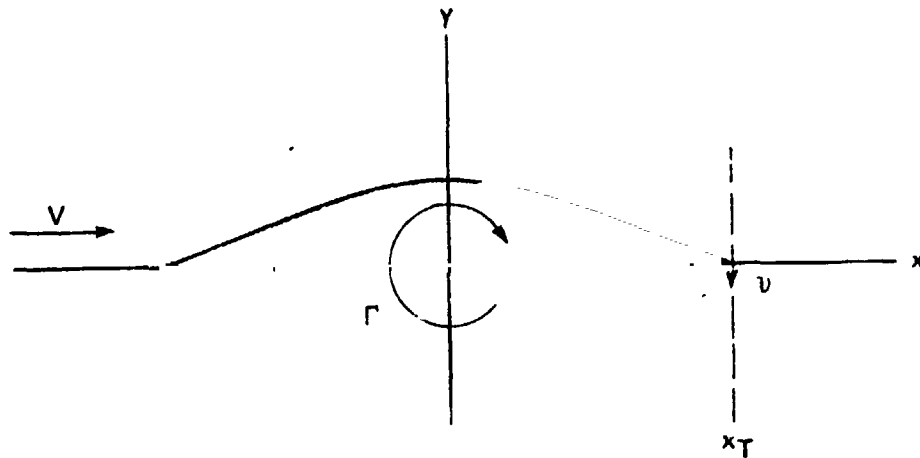
$$\text{VELOCITY POTENTIAL} = Vx + \frac{\Gamma}{2\pi} \tan^{-1}\left(\frac{y}{x}\right) \tag{A1}$$

$$\text{DOWNWASH VELOCITY} = \frac{\partial \phi}{\partial y} = \frac{\Gamma}{2\pi x_T}\left[\frac{1}{1 + (y/x_T)^2}\right]$$

$$= v_{max}\left[\frac{1}{1 + (y/x_T)^2}\right] \tag{A2}$$

$$V_x = V\left[1 - \frac{\sin^2\alpha}{1 + (y/x_T)^2}\right]$$

$$v = V\left[\frac{\sin\alpha \cos\alpha}{1 + (y/x_T)^2}\right]$$

$$d\ell = \rho V_x v \, dy$$

$$\ell = \rho V^2 \sin\alpha \cos\alpha \, x_T^2\left[\int_{-\infty}^{\infty} \frac{dy}{x_T^2 + y^2} - x_T^2 \sin^2\alpha \int_{-\infty}^{\infty} \frac{dy}{(x_T^2 + y^2)^2}\right] \tag{A3}$$

$$c_\ell = 2\pi \sin\alpha \cos^2\alpha \left(1 - \frac{\sin^2\alpha}{2}\right) \tag{A4}$$

$$\frac{dc_\ell}{d\alpha} = \pi \cos\alpha \, (^{\sim} \sin^4\alpha + 2\cos^2\alpha - 4\sin^2\alpha - 3\sin^2\alpha \cos^2\alpha) \tag{A5}$$

22

$$c_d = c_\ell \tan\alpha \tag{A6}$$

The nonpotential lift equation (A4) and its derivative provide the basis for the estimation of lift characteristics for sharp airfoils and for blunt airfoils at transonic and supersonic speeds. The equations for zones 3 through 6 incorporate multiplying factors to account for compressibility, sweep, aspect-ratio transformations, and detached bow shocks.

Angle of Attack ν_E

The angle of attack for the onset of the leading-edge limit Mach number, equation (A11), is found by equating equations (A7) and (A10). Equation (A7) is the solution to the curvilinear, compressible, potential flow around a parabolic leading-edge presented in reference 14. Equation (10) stems from the substitution of the limit Mach number (A9) into the general isentropic equation (A8). Equation (A11) is fitted to various families of airfoils for which the leading-edge radius-to-chord ratio can be expressed in terms of the thickness-to-chord ratio.

$$\left(\frac{V_e}{V_\infty}\right)_{MAX} = \sqrt{1 + \left(1 + \sqrt{\frac{r/c}{2}}\right)^2 \left(\frac{2\alpha^2}{r/c}\right)} \tag{A7}$$

$$\left(\frac{V_e}{V_\infty}\right) = \frac{M_e \sqrt{1 + \left(\frac{\gamma-1}{2}\right)M^2}}{M \sqrt{1 + \left(\frac{\gamma-1}{2}\right)M_e^2}} \qquad \text{SET } M_e = \sqrt{\frac{\gamma+3}{2}} \tag{A8, A9}$$

$$\left(\frac{V_e}{V_\infty}\right)_{MAX} = 1.236 \sqrt{0.2 + \frac{1}{M^2}} \tag{A10}$$

$$\alpha_e = \frac{\sqrt{1.528 - 0.695 M^2}}{M\left(1 + \sqrt{\frac{2}{r/c}}\right)} \tag{A11}$$

Wings of Aspect Ratio Below 2

The nonpotential lift equations are used for all sharp wings. For aspect ratios below 2, the account for aspect ratio differs from the Prandtl transformation and assumes values taken from reference 15 (fig. 4) and reference 16 (fig. 6).

$$C_L = \sin\alpha \cos^2\alpha \left(1 - \frac{\sin^2\alpha}{2}\right)\left(\frac{S_x}{S_{WING}}\right)(F_{INT})\left[\sqrt{ARWX} - (2 - ARWX)\tan\alpha\right] \tag{A12}$$

$$\frac{dC_L}{d\alpha} = \left[\sqrt{ARWX}\,(2 - 9\sin^2\alpha + 5\sin^4\alpha)\cos\alpha + (2 - ARWX)(4 - 10\sin^2\alpha + 5\sin^4\alpha)\right]\left(\frac{S_x}{S_{WING}}\right)\left(\frac{F_{INT}}{2}\right) \tag{A13}$$

For Mach numbers above 2, multiply the above equations by $\left(.5 + \dfrac{.866}{\sqrt{M^2-1}}\right)$

Equation (A12) for wings alone (ARW=ARWX) can be reduced to the intuitive "leading-edge suction analogy" equation devised by Polhamus (ref. 15), when the term $\dfrac{\sin^2\alpha}{2}$ is omitted.

$$C_L = \sqrt{ARW}\ \sin\alpha\cos^2\alpha + (2 + ARW)\ \sin^2\alpha\cos\alpha$$

This is the same as equation 4 of reference 15, the sum of the so-called potential and vortex lift components.

$$C_L = K_p \sin\alpha\cos^2\alpha + K_v \sin^2\alpha\cos\alpha$$

(Ref. 15)

Camber Drag

The camber input, CLO, in AEROX is the actual lift coefficient at zero angle of attack. The incremental drag coefficient, CDCAM, produced by the camber is evaluated on the basis of a constant value of the maximum lift-to-drag ratio for the assumed parabolic polar curves for the related symmetrical and cambered airfoils.

$$C_{DCAM} = \frac{C_{L_0}}{(L/D)_{max}} = 2C_{L_0}\sqrt{\frac{C_{D_0}}{\pi\,ARW}} \tag{A-14}$$

CDC is the minimum drag coefficient of the symmetrical wing, and is one of the optional AEROX inputs for each Mach number, when the control integer ICDO = 1. When CDO is not specified, and the integer ICDO = 0, CDCAM = CLO/20.

The parameter CLO, representing wing camber, is attenuated to zero in AEROX, when the sonic leading-edge condition is reached. If finite values of lift coefficient are to be retained at supersonic speeds, they are input as CLOB values for each Mach number in the array. (See the shuttle test case in Vol. II).

APPENDIX B - HORIZONTAL TAIL

Downwash

The equations describing the downwash field used in the TRIMDG routine are based on a correlation of theory and data from references 17 through 20.

Wake angle,

$$\text{EPSD} = \alpha \left[\frac{3.9 - \text{ARW}^{3-\text{ARW}}}{3\sqrt{1+\text{TRW}}}\right]\left[\frac{2.}{\text{ARW}} + 0.1\left(\sqrt{\frac{2\,\text{SPANW}}{3.\text{CBARW}}} + \sqrt{\frac{\text{SPANW}}{Z\,L_T}}\right)\right] \qquad (B1)$$

Nondimensionalized offset distance from tail to wake,

$$\left|\frac{2.Y}{\text{SPANW}}\right| = \left|\frac{2.Y_{\text{HOR}}}{\text{SPANW}} + \left(\frac{2.L_T}{\text{SPANW}} - \frac{1.5}{\text{ARW}}\right)\sin(\text{EPSD}) - \frac{2.L_T}{\text{SPANW}}\sin\alpha\right| \qquad (B2)$$

Downwash angle at the horizontal tail,

$$\text{DWASH} = \alpha\left[\frac{3.9 - \text{ARW}^{3-\text{ARW}}}{9.\sqrt{1+\text{TRW}}}\right]\left[0.2\sqrt{\frac{2\,\text{SPANW}}{L_T}} + \frac{2.}{\text{ARW}}\right]\left[2.+\cos\frac{9}{4}\alpha\right]\left[1.-\frac{3}{2}\left|\frac{2Y}{\text{SPANW}}\right|\right] \qquad (B3)$$

Downwash derivative with respect to angle of attack, $d\epsilon/d\alpha$,

$$\text{DEPDA} = \left[\frac{3.9 - \text{ARW}^{3-\text{ARW}}}{9\sqrt{1+\text{TRW}}}\right]\left[0.2\sqrt{\frac{2\,\text{SPANW}}{L_T}} + \frac{2}{\text{ARW}}\right]\left[1.-\frac{3}{2}\left|\frac{2Y}{\text{SPANW}}\right|\right]\left[2.+\cos\frac{9}{4}\alpha - \frac{9}{4}\alpha\sin\frac{9}{4}\alpha\right] \qquad (B4)$$

Supersonic downwash attenuation factor; if 1<M, multiply (B3) and (B4) by ATENF.

$$\text{ATENF} = 1.-0.1\sqrt{M^2-1}\left[1+\frac{\tan(\text{SWPWLE})}{\frac{2}{\text{ARW}} + \frac{2L_T}{\text{SPANW}}}\right]$$

26

Horizontal-Tail Aerodynamics

The increments in lift coefficient (based on SWING) contributed by an aft horizontal tail are evaluated by the nonpotential lift equations. For subsonic speeds ($Z \leq 4$),

$$C_{L_{HOR}} = (CPMXS+1) \pi \sin\alpha_H \cos^2\alpha_H \left(1 - \frac{\sin^2\alpha_H}{2}\right)\left(\frac{ARH}{ARH+2}\right)\left(\frac{S_{HOR}}{SWING}\right) \cos(DWASH)\cos(SQH) \qquad (B5)$$

at supersonic speeds ($Z = 5,6$), the nonpotential lift for the wing is multiplied by suitable ratios of the geometry to obtain the tail lift coefficient.

$$C_{L_{HOR}} = C_{L_W} \left(\frac{ARH}{ARW}\right)\left(\frac{ARW+2}{ARH+2}\right)\left(\frac{COS(SWPW)}{COS(SQH)}\right)\left(\frac{SHOR}{SWING}\right)\left(\frac{\alpha_H}{\alpha}\right) COS(DWASH) \qquad (B6)$$

$$\alpha_H = \alpha - DWASH + IT$$

The induced drag coefficient contributed by the horizontal tail is positive for either up or down tail loads.

$$C_{D_{HOR}} = \left| C_{L_{HOR}} TAN(\alpha+IT) \right| \qquad (B7)$$

Pitching-Moment Coefficient and Stability

The pitching-moment coefficient includes the separate contributions of the body, wing and horizontal tail. Initial values of CMO for the wing and CMOB for the body may be input. The wing pitching moment includes the components from the upper and lower surfaces and from the chord extension or strake. For the transonic limit-shock conditions in flow zone 4, the wing upper-surface contributions are further divided into the separate loadings upstream and downstream of the limit shock for both shock geometries covered by IXCD= 0, 1.

27

$$C_M = C_{MO} + C_{M_{NOSE}} + \frac{(CLWU)(EU) + (CLWL)(EL)}{CBARW(\cos \alpha)} + (CLW)(FMEX) + \frac{(C_{L_{HOR}})(LE)}{CBARW(\cos \alpha)} \qquad (B8)$$

The offsets EU and EL of the wing surface loadings from the moment center are defined for each flow zone Z.

The static longitudinal stability derivative includes the wing and tail components (neglects the body derivative).

$$CMCL = \frac{dC_M}{dC_L} = \frac{\left(\frac{dC_{Lw}}{d\alpha}\right)\left(\frac{FMEX - EBAR}{1 + FLEX}\right) - \left(\frac{dC_{L_{HOR}}}{d\alpha_H}\right)(1 - DEPDA)(LE)}{CBARW(\cos \alpha)\left[\frac{dC_{Lw}}{d\alpha} + \left(\frac{dC_{L_{HOR}}}{d\alpha_H}\right)(1 - DEPDA)\right]} \qquad (B9)$$

FLEX and FMEX are the lift and pitching-moment factors for the wing chord extension, EBAR is the effective eccentricity of the wing center of lift, and LE is the tail length from the reference moment center (usually CG).

Longitudinal Trim (ITRIM=1)

The AEROX program includes an option for evaluating the trimmed values of lift and drag coefficients. For angles of attack up to 25°, the trim function is performed while maintaining a constant value of lift coefficient. Thus, the angle of attack is adjusted to compensate for the changes in tail lift accompanying deflection of the tail to trim out the pitching-moment (CM).

The horizontal tail deflection to trim while maintaining constant total lift coefficient with adjustment of the angle of attack is,

$$DELH = \frac{CM}{\left(\frac{dC_{L_{HOR}}}{d\alpha_H}\right)\left(\frac{LE}{CBARW(\cos \alpha)} + CMCL\right)} = \frac{DCLTR}{\left(\frac{dC_{L_{HOR}}}{d\alpha_H}\right)} \qquad (B10)$$

28

DCLTR is the increment in lift coefficient produced by the tail deflection DELH. It is recovered through the adjustment in angle of attack, where,

$$\alpha_{TRIM} = \alpha - \frac{DCLTR}{\frac{dC_{L_W}}{d\alpha} + \frac{dC_{L_{HOR}}}{d\alpha_H}\left(1 - DEPDA\right)} \tag{B11}$$

The incremental drag coefficient DCDTR accompanying the trim process at constant lift coefficient is the sum of the increments of induced drag coefficients for the wing and tail.

$$DCDTR = \frac{C_{L_W}^2 - \left(C_{L_W} + DCLTR\right)^2}{\pi ARW} + \left[\frac{\left(C_{L_{HOR}} + DCLTR\right)^2 - C_{L_{HOR}}^2}{\pi ARH}\right]\left(\frac{S_{WING}}{S_{HOR}}\right) \quad (z=2) \tag{B12}$$

$$DCDTR = -DCLTR\left(\tan\alpha\right)^{DEXP} + DCLTR\left[\tan\left(\alpha_{TRIM} + I_T + DELH\right)\right] \quad (3 \leq z) \tag{B13}$$

For angles of attack above 25°, AEROX performs the longitudinal trim at constant angle of attack, $\alpha_{TRIM} = \alpha$.

$$DCLTR = CM\left(\frac{CBARW}{LE}\right)\cos\alpha$$

$$DELH = \frac{DCLTR}{\left(\frac{dC_{L_{HOR}}}{d\alpha_H}\right)\cos(DWASH)}$$

$$DCDTR = \left\{\frac{\left[C_{L_{HOR}} + \frac{DCLTR}{\cos(DWASH)}\right]^2 - C_{L_{HOR}}^2}{\pi ARH}\right\}\left(\frac{S_{WING}}{S_{HOR}}\right) \quad (z=2)$$

$$DCDTR = DCLTR\ \tan\left(\alpha + I_T + DELH\right) \quad (3 \leq z)$$

Care should be exercised in interpreting the trimmed characteristics. For example, if the stability is too large, the tail deflections to trim may exceed realistic limits for horizontal tail deflections. The tail angles of attack, α_H, should be kept below 40°.

APPENDIX C - BODY (BCLCD1 Subroutine)

The aerodynamic normal force on the body is estimated by the equation summing the slender-body contribution and the viscous cross-flow drag. An updated discussion of the approach appears in reference 21, which was the principal source of the values used for constructing the contour plot of cross-flow drag coefficient against cross-flow Reynolds number and cross-flow Mach number shown in figure 3. The BCLCD1 subroutine contains explicit equations for each of the nine regions indicated. The Reynolds numbers are calculated using the atmosphere properties subroutine AT62.

$$CN_{NOSE} = \left[\sin 2\alpha \cos \frac{\alpha}{2} (ASECT) + CDC(ETAN) \sin^2\alpha \, (APLAN) \right] \Big/ SWING \tag{C1}$$

$$CL_{NOSE} = CN_{NOSE} \cos\alpha + CLOB \tag{C1A}$$

$$CD_{NOSE} = CN_{NOSE} \sin\alpha + CDOB \tag{C1B}$$

$$CM_{NOSE} = CN_{NOSE} \left(\frac{XCG - 0.6\,XLN}{CBARW} \right) + CMOB \tag{C2}$$

At supersonic speeds, X=5,6), the afterbody load is included, for exposed le.··rh ΔX_{AFT}.

$$CN_{BODY} = CN_{NOSE} \left(1 + \frac{\Delta X_{AFT}}{XLN} \right) \left(\frac{M-1}{M} \right) \tag{C3}$$

$$CM_{BODY} = CM_{NOSE} - \left(\frac{CN_{AFT}}{CBARW} \right) \left(XLB - \frac{\Delta X_{AFT}}{2} - XCG \right) \tag{C4}$$

The finite length factor, ETAN, (from a curve fit to ref. 21) is:

$$ETAN = 0.55 + \frac{XLN}{90(BDMAX)}$$

The slender-body and cross-flow approach formed the basis for the method presented in reference 22.

References

1. Smith, A. M. O., "High-Lift Aerodynamics", 1974 Wright Brothers Lecture, AIAA Journal of Aircraft, Vol. 12, No. 6, June 1975, pp 501-538.

2. Laitone, E. V., "Limiting Velocity by Momentum Relations for Hydrofoils Near the Surface and Airfoils in Near Sonic Flow", Proceedings of the Second U. S. National Congress of Applied Mechanics, June 14-18, 1954, pp 751-753.

3. Laitone, E. V., "Local Supersonic Region on a Body Moving at Subsonic Speeds", Symposium Transonicum, Aachen, Germany, September 3-7, 1962, Edited by Klaus Oswatitsch.

4. Axelson, John A., "Estimation of Transonic Aircraft Aerodynamics to High Angles of Attack", AIAA Paper No. 75-996, August 1975.

5. Nelms, W. P. and Axelson, J. A., "Preliminary Performance Estimates of a Highly Maneuverable Remotely Piloted Vehicle", NASA TN D-7551, Feb. 1974.

6. Levin, A.D., Castellano, C.R., and Hague, D.S., "High Performance Dash on Warning Air Mobile Missile System", NASA TMX-62,479, Sept., 1975.

7. Nelms, W. P., Murphy, R., and Barlow, A., "Preliminary Analysis of Long-Range Aircraft Designs for Future Heavy Airlift Missions", NASA TMX-73,131, June, 1976.

8. Vanderplaats, G. N.: "CONMIN - A Fortran Program for Constrained Function Minimization", NASA TMX-62,282, August 1973.

9. Flax, Alexander H.: Comment on "Simplification of the Wing-Body Problem", AIAA Journal of Aircraft, Vol. 10, no. 10, October 1973, pp. 640.

10. Flax, Alexander H.: Comment on "Correlation of Wing-Body, Combination Lift Data", AIAA Journal of Aircraft, vol. 11, No. 5, May 1974, pp. 303-304

11. Ames Research Staff, "Equations, Tables and Charts for Compressible Flow" NACA TR 1135, 1953.

12. Cleary, J. W., and Axelson, J. A., "Theoretical Aerodynamic Characteristics of Sharp and Circularly Blunt-Wedge Airfoils at Hypersonic Speeds" NASA TR R-202, July 1964.

13. Mayer, J. P., "A Limit Pressure and an Estimation of Limit Forces on Airfoils at Supersonic Speeds" NACA RM L8F23, 1948.

14. Ericsson, L. E., and Reding, J. P., "Stall-Flutter Analysis", Journal of Aircraft, AIAA, vol. 10, Jan. 1973.

15. Polhamus, E. C., "Predictions of Vortex-Lift Characteristics by a Leading-edge Suction Analogy", Journal of Aircraft, AIAA, vol. 8, April 1971.

16. Mendenhall, M. R., and Nielsen, J. N., "Effect of Symmetrical Vortex Shedding on the Longitudinal Aerodynamic Characteristics of Wing-Body-Tail Combinations", NASA Contract NAS2-7347, Nielsen Engineering and Research TR69, May 1974.

17. Silverstein, A., and Katzoff, S., "Design Charts for Predicting Downwash Angles and Wake Characteristics Behind Plain and Flapped Wings", NACA TR-648, 1939.

18. Perkins, C. D., and Hage, R. E., "Airplane Performance, Stability and Control", John Wiley and Sons, New York, 1949.

19. Axelson, J. A., "Downwash Behind a Triangular Wing of Aspect Ratio 3 - Transonic Bump Method", NACA RM A53I23, 1953.

20. Decker, J. L., "Prediction of Downwash at Various Angles of Attack for Arbitrary Tail Locations", Aeronautical Engineering Review, August 1956, pp 22-27.

21. Jorgenson, L. H., "Prediction of Static Aerodynamic Characteristics for Space Shuttle-like and Other Bodies at Angles of Attack from 0° to 180°" NASA TN D-6996, 1973.

22. Saffell, B. F., Millard, L. H. and Brooks, E. N., "A Method for Predicting the Static Aerodynamic Characteristics of Typical Missile Configurations for Angles of Attack to 180 degrees", Naval Ship Research and Development Center Report 3645, 1971.
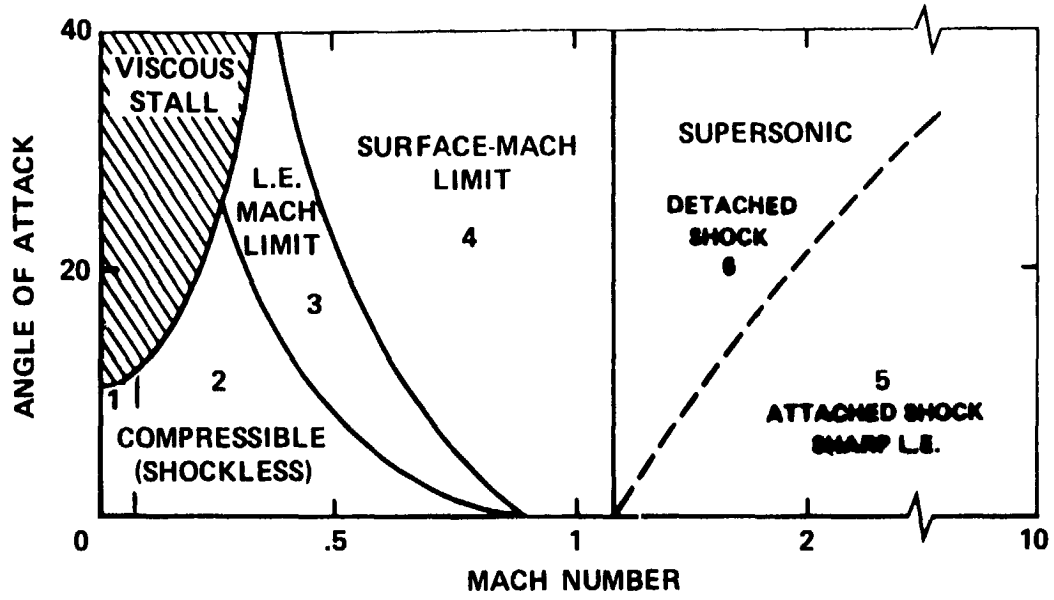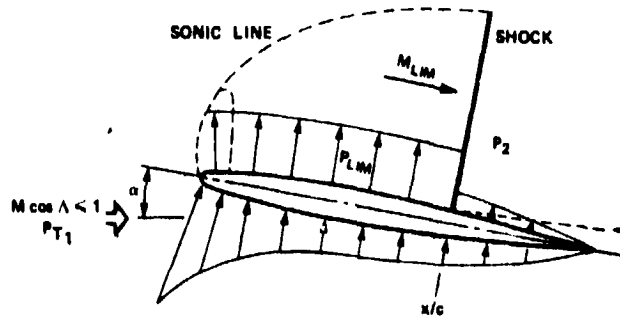
Fig.1. Flow zones.

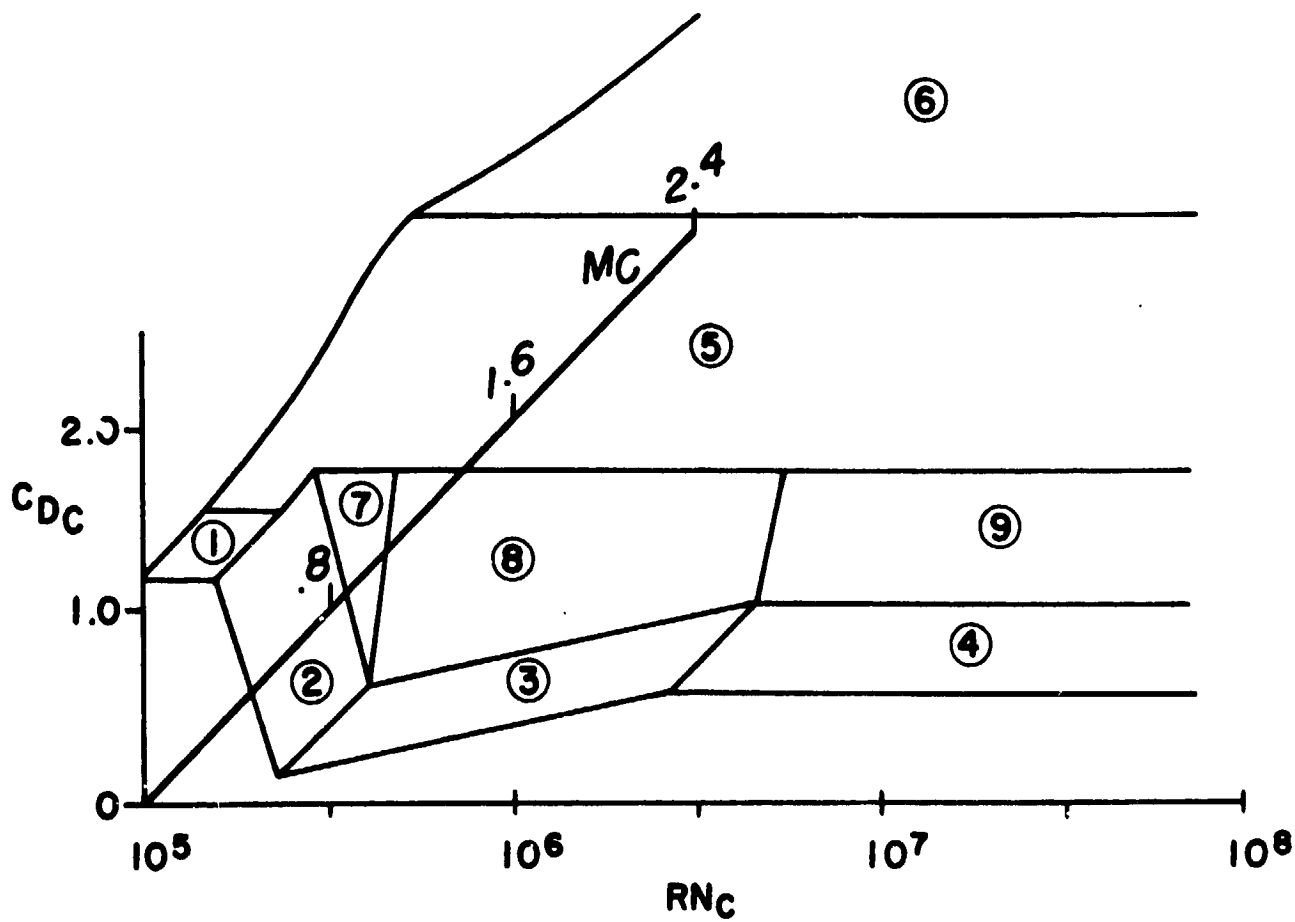Fig. 2. Surface Mach-number limited transonic flow.

FIGURE 3.- CONTOUR OF CROSS-FLOW DRAG COEFFICIENT WITH CROSS-
FLOW MACH AND REYNOLDS NUMBERS.